

On the Construction of the BGK-Type Schemes for Compressible Flow Simulations

by

K. Xu, C. Kim, L. Martinelli, and A. Jameson
Princeton University, Princeton, New Jersey, USA

Proceedings

6th International Symposium on Computational Fluid Dynamics

Lake Tahoe
September 1995

On the Construction of BGK-Type Schemes for Compressible Flow Simulations

Kun Xu, Chongam Kim, Luigi Martinelli and Antony Jameson
Department of Mechanical and Aerospace Engineering
Princeton University, Princeton, NJ 08544

1 Introduction

The development of numerical methods based on gas-kinetic theory started in the earlier 1970s. The first scheme of this class which is widely used in the astrophysical community is the beam scheme [11]. This scheme is based on the collisionless Boltzmann equation, where the left and right moving particles generated from the equilibrium states in each side could penetrate through the cell interface to form the numerical fluxes. Beginning in the 1980's, the beam scheme was "re-invented", modified or extended by many authors. Pullin was the first one to use the complete error function to get the numerical fluxes and the scheme is named Equilibrium Flux Method (EFM). By applying the Courant-Isaacson-Reeves (CIR) upwind technique directly to the collisionless Boltzmann equation, Deshpande derived a similar scheme which is named Kinetic Flux Vector Splitting (KFVS). Combining both the multidimensional technique and the KFVS, Eppard and Grossman developed several versions of first order multidimensional gas-kinetic schemes [4].

In order to capture the gas evolution process more precisely, a new class of gas-kinetic schemes based on the collisional BGK model has been recently proposed [8, 12, 13]. We will refer to this class of schemes as BGK-type to distinguish them from other gas-kinetic schemes based on the collisionless Boltzmann equation. In our approach, the full integral solution of the BGK model is used locally to get the time-dependent gas distribution function at the cell interface. BGK-type schemes of this class yield the Navier-Stokes equations directly, and have many advantages over most centered and upwind schemes [13].

In this paper, we propose an alternative formulation which improves upon existing BGK-type schemes. In particular, characteristic variables are used in the reconstruction step, and discontinuous slopes of the equilibrium state g are allowed. Section 2 describes the basic scheme in terms of the reconstruction and gas evolution approach. Section 3 includes some numerical examples which indicates the merits of the proposed approach.

2 The BGK-Type Schemes for the Navier-Stokes Equations

2.1 Reconstruction

In the reconstruction stage, the cell averaged value U_j can be interpolated as

$$\bar{U}_j(x) \quad \text{for } x_{j-1/2} \leq x \leq x_{j+1/2},$$

and the interpolation principles could be TVD, ENO or LED [6]. The interpolated value of $\bar{U}_j(x)$ used in this paper is the characteristic variable, from which the conservative variables in each cell can be

derived and denoted as mass $\bar{\rho}_j(x)$, momentum $\bar{P}_j(x)$ and energy $\bar{\epsilon}_j(x)$. For the BGK type flow solver, the interpolated pointwise values as well as linear slopes of the conservative variables inside each cell will be used to evaluate the time-dependent gas distribution functions at the cell interface.

2.2 The BGK Solver

For a one-dimensional flow the BGK model is

$$f_t + uf_x = \frac{g - f}{\tau}, \quad (1)$$

where f is the gas distribution function and g is the corresponding distribution of the equilibrium state which f approaches. Both f and g are functions of space x , time t , particle velocity u and internal degrees of freedom ξ . The equilibrium state is described by a Maxwellian distribution $g = \rho(\frac{\lambda}{\pi})^{\frac{K+1}{2}} e^{-\lambda((u-U)^2 + \xi^2)}$ where ρ is the density and U is the macroscopic velocity. The internal degrees of freedom of ξ is given by $K = (5 - 3\gamma)/(\gamma - 1) + 2$ in the one-dimensional case when the particle motion in the y and z directions is included as internal motion. The relations between mass ρ , momentum P and energy ϵ densities with the distribution function f can be written as

$$\begin{pmatrix} \rho \\ P \\ \epsilon \end{pmatrix} = \int \psi_\alpha f d\Xi, \quad \alpha = 1, 2, 3 \quad (2)$$

where ψ_α is the vector of moments $\psi_\alpha = (1, u, \frac{1}{2}(u^2 + \xi^2))^T$ and $d\Xi = dud\xi$ is the volume element in phase-space. Since mass, momentum and energy are conserved in particle collisions, f and g have to satisfy the conservation constraint of

$$\int (g - f) \psi_\alpha d\Xi = 0, \quad \alpha = 1, 2, 3 \quad (3)$$

at any point in space and time. To the first order of τ , the distribution function f can be written as $f = g - \tau(g_t + ug_x)$. Taking moments ψ_α to the BGK equation, we can get the Navier-Stokes equations.

The general solution of f at the cell interface $x_{j+1/2}$ and time t is

$$f(x_{j+1/2}, t, u, \xi) = \frac{1}{\tau} \int_0^t g(x', t', u, \xi) e^{-(t-t')/\tau} dt' + e^{-t/\tau} f_0(x - ut), \quad (4)$$

where $x' = x_{j+1/2} - u(t - t')$ is the trajectory of a particle motion and f_0 is the initial nonequilibrium distribution function f at the beginning of each time step ($t = 0$). Generally, f_0 and g around the cell interface $x_{j+1/2}$ are assumed to be

$$f_0 = \begin{cases} g^l (1 + a^l(x - x_{j+1/2})), & x \leq x_{j+1/2} \\ g^r (1 + a^r(x - x_{j+1/2})), & x \geq x_{j+1/2} \end{cases} \quad (5)$$

and

$$g = g_0 \left(1 + (1 - H[x - x_{j+1/2}]) \bar{a}^l(x - x_{j+1/2}) + H[x - x_{j+1/2}] \bar{a}^r(x - x_{j+1/2}) + \bar{A}t \right). \quad (6)$$

Here g^l, g^r and g_0 are local Maxwellian distribution functions, which are located at the left, right and middle of a cell interface, and $H[x]$ is the Heaviside function. Notice that in the present approach we allow for discontinuous slopes of g . The dependence of a^l, a^r, \dots, \bar{A} on the particle velocity can be obtained from the Taylor expansion of g_0 and have the forms of $a^l = a_\alpha^l \psi_\alpha, \dots, \bar{A} = \bar{A}_\alpha \psi_\alpha$, where all coefficients of $a_1^l, a_2^l, \dots, \bar{A}_3$ are local constants.

In the reconstruction stage, we have obtained $\bar{\rho}_j(x)$, $\bar{P}_j(x)$ and $\bar{\epsilon}_j(x)$ in each cell $x_{j-1/2} \leq x \leq x_{j+1/2}$ from the interpolation of the characteristic variables. By using the relation between the gas distribution function f_0 and the macroscopic variables (Eq.(2)), we get

$$\int g^l \psi_\alpha d u d \xi = \begin{pmatrix} \bar{\rho}_j(x_{j+1/2}) \\ \bar{P}_j(x_{j+1/2}) \\ \bar{\epsilon}_j(x_{j+1/2}) \end{pmatrix} ; \quad \int g^l a^l \psi_\alpha d u d \xi = \begin{pmatrix} \frac{\bar{\rho}_j(x_{j+1/2}) - \bar{\rho}_j(x_j)}{\Delta x^-} \\ \frac{\bar{P}_j(x_{j+1/2}) - \bar{P}_j(x_j)}{\Delta x^-} \\ \frac{\bar{\epsilon}_j(x_{j+1/2}) - \bar{\epsilon}_j(x_j)}{\Delta x^-} \end{pmatrix},$$

similar equations can be found for g^r and a^r . Here, $\Delta x^- = x_{j+1/2} - x_j$ is the distance of the center from the cell interface. From the above equations g^l and g^r as well as a^l and a^r in f_0 can be completely determined.

After determining f_0 , the equilibrium distribution function g_0 at $(x = 0, t = 0)$ can be found from

$$\int g_0 \psi_\alpha d \Xi = \int_{u>0} \int g^l \psi_\alpha d \Xi + \int_{u<0} \int g^r \psi_\alpha d \Xi, \quad \alpha = 1, 2, 3. \quad (7)$$

The moments of g_0 in the above equation correspond to the mass ρ_0 , momentum P_0 and energy ϵ_0 densities at $(x = 0, t = 0)$. Then, \bar{a}^l and \bar{a}^r in g can be obtained from the following formula

$$\int g_0 \bar{a}^l \psi_\alpha d u d \xi = \begin{pmatrix} \frac{\rho_0 - \bar{\rho}_j(x_j)}{\Delta x^-} \\ \frac{P_0 - \bar{P}_j(x_j)}{\Delta x^-} \\ \frac{\epsilon_0 - \bar{\epsilon}_j(x_j)}{\Delta x^-} \end{pmatrix} ; \quad \int g_0 \bar{a}^r \psi_\alpha d u d \xi = \begin{pmatrix} \frac{\bar{\rho}_{j+1}(x_{j+1}) - \rho_0}{\Delta x^+} \\ \frac{\bar{P}_{j+1}(x_{j+1}) - P_0}{\Delta x^+} \\ \frac{\bar{\epsilon}_{j+1}(x_{j+1}) - \epsilon_0}{\Delta x^+} \end{pmatrix},$$

where $\Delta x^+ = x_{j+1} - x_{j+1/2}$.

After substituting Eq.(5) and Eq.(6) into Eq.(4), the final gas distribution function at a cell interface is

$$\begin{aligned} f(x_{j+1/2}, t, u, \xi) &= (1 - e^{-t/\tau}) g_0 + \left(\tau(-1 + e^{-t/\tau}) + t e^{-t/\tau} \right) \left(\bar{a}^l H[u] + \bar{a}^r (1 - H[u]) \right) u g_0 \\ &\quad + \tau(t/\tau - 1 + e^{-t/\tau}) \bar{A} g_0 + e^{-t/\tau} f_0(-ut), \end{aligned}$$

with

$$f_0(-ut) = \begin{cases} g^l(1 - a^l ut), & u \geq 0 \\ g^r(1 - a^r ut), & u \leq 0. \end{cases}$$

The only unknown term \bar{A} in the above equation can be obtained from

$$\int_0^T \int (g - f) \psi_\alpha d t d \Xi \big|_{x=x_{j+1/2}} = 0.$$

Finally, the time-dependent numerical fluxes in the x -direction across the cell interface are computed as:

$$\begin{pmatrix} \mathcal{F}_\rho \\ \mathcal{F}_P \\ \mathcal{F}_\epsilon \end{pmatrix}_{j+1/2} = \int u \begin{pmatrix} 1 \\ u \\ \frac{1}{2}(u^2 + \xi^2) \end{pmatrix} f(x_{j+1/2}, t, u, \xi) d u d \xi.$$

Positivity Condition: The BGK-type schemes provide an alternative gas evolution model in contrast to the classical Riemann solver. From Eq.(7), we know that g_0 has positive density and temperature if g^l and g^r obtained in the reconstruction stage are physical states with positive density and temperature. Thus $g_0 > 0$ is satisfied and all particles have positive probability. If we ignore all slopes in the BGK-type schemes, the distribution function f at the cell interface could be simplified as

$$f(x_{j+1/2}, t) = (1 - e^{-t/\tau}) g_0 + e^{-t/\tau} f_0.$$

Since $g_0 > 0, f_0 > 0$ and $e^{-t/\tau} < 1$, f is strictly positive ($f > 0$). Therefore, f has positive density and temperature, since

$$\int f du > 0 \quad \text{and} \quad \int u^2 f du - \frac{(\int u f du)^2}{\int f du} > 0. \quad (8)$$

We define Eq.(8) as the positivity condition for the BGK schemes. Roe's approximate Riemann solver cannot guarantee that the solutions of the flow variables at the cell interface satisfy this condition [10]. Multidimensional Property: For two dimensional flow, the BGK model is

$$f_t + u f_x + v f_y = (g - f)/\tau,$$

which yields the 2D Navier-Stokes equations of

$$W_t + A W_x + B W_y = S.$$

It is well known that the matrices A and B do not commute. This yields the necessity of wave modelling for the development of multidimensional upwind schemes. However, since in the gas-kinetic model the particle velocities are independent variables, BGK-type schemes extends transparently to multi-dimensions.

3 Numerical Examples

Case(1). Reference [7] presents the analysis of a BGK scheme for the advection equations. By applying the new numerical discretization in this paper, the similar BGK-type scheme for the linear advection-diffusion equation can be obtained. Fig.(1) shows the results of a decaying sinusoidal wave after one period time ($t = 2.0$) using 40 cells and an ENO reconstruction for the cell interface values, where CFL time step is 0.1 and $Re(\equiv cL/\nu)$ is 400. Compared to the results of [2], higher order (more than second order) results are almost identical, while first order and second order results of the BGK-type schemes are much better.

Case(2). The Shu-Osher test case consists of a moving shock with Mach number 3 interacting with sine waves. As observed by many authors, MUSCL type TVD schemes present very smeared results for the density distribution. Fig.(2) shows the density distribution computed on 400 points using the BGK solver and a 4th-order ENO [5] interpolation for the discrete values at the cell interface. The results confirm the accuracy of the flow solver and the necessity of higher order reconstruction for this test case.

Case(3). In order to validate the applicability of the present BGK-type scheme for the flow calculations with both strong shocks and high expansion regions, an impulsively started cylinder with initial Mach number of 3 is chosen. This problem is particularly difficult because the very wide expansion in the rear part of cylinder produces a vacuum-like low density region. Most upwind schemes have difficulties in maintaining positive pressure and/or density, and generally require "*ad hoc fixes*" to overcome this problem. The present BGK scheme, however, doesn't exhibit any particular difficulties and preserves positivity. Both the first order and second order schemes are successfully applied in this case. Fig.(3) shows density contours at $t = 4.0$. The curved shock is nicely captured with two interior points and the V-shaped weak shock induced by the expansion at the rear part of cylinder is also reproduced correctly.

4 Conclusion

Both the initial reconstruction of the data and the gas evolution stage can affect the accuracy and robustness of a numerical scheme. The BGK model provides an alternative gas evolution model for the

Navier-Stokes equations and allows the construction of numerical methods which have many advantages over more classical Godunov-type schemes, especially for hypersonic unsteady flow calculations.

References

- [1] P. L. Bhatnagar, E. P. Gross, M. Krook, *Phys. Rev.* , **94**, 511 (1954)
- [2] C. Chiu and X. Zhong, "Simulation of Transient Hypersonic Flow Using the ENO Schemes", AIAA-95-0469, 33rd Aerospace Sciences Meeting and Exhibit, 1995.
- [3] S.M. Deshpande, "A Second Order Accurate, Kinetic-Theory Based, Method for Inviscid Compressible Flows," NASA Langley Tech. paper No. 2613, 1986.
- [4] W. Eppard and B. Grossman, "A multidimensional kinetic-based upwind solver for the Euler equations", AIAA 11th Computational Fluid Dynamics Conference, Orlando, FL, July, 1993.
- [5] A. Harten, B. Engquist, S. Osher and S. Chakravarthy, "Uniformly High Order Accurate Essentially Non-Oscillatory Schemes, III", *J. Comput. Phys.*, **71**, 231-303, 1987.
- [6] A. Jameson, "Analysis and Design of Numerical Schemes for Gas Dynamics 1 Artificial Diffusion, Upwind Biasing, Limiters and their Effect on Accuracy and Multigrid Convergence" to appear in *International Journal of Computational Fluid Dynamics*, 1994.
- [7] C.A. Kim, K. Xu, L. Martinelli and A. Jameson, "The Gas-kinetic BGK Scheme for Computational Gas Dynamics Applied to Advection Equations", submitted to *Int. J. Num. Met. in Fluids*, Jan. 1995.
- [8] K.H. Prendergast and K. Xu , "Numerical Hydrodynamics from Gas-Kinetic Theory", *J. of Comput. Phys.* **109**, 53, 1993.
- [9] D.I. Pullin, "Direct Simulation Methods for Compressible Inviscid Ideal Gas Flow", *J. of Comput. Phys.* **34**, 231-244 (1980).
- [10] P. L. Roe, "Approximate Riemann Solvers, Parameter Vectors and Difference Schemes", *J. Comput. Phys.*, **43**, 357, 1981.
- [11] R. H. Sanders and K. H. Prendergast, "The possible relation of the three-kiloparsec arm to explosions in the galactic nucleus," in *Astrophysical Journal*, **188**, 1974.
- [12] K. Xu and K.H. Prendergast, "Numerical Navier-Stokes Solutions from Gas-Kinetic Theory", *J. Comput. Phys.*, **114**, 9-17, 1994.
- [13] K. Xu , L. Martinelli and A. Jameson, "Gas-Kinetic Finite Volume Methods, Flux-Vector Splitting and Artificial Diffusion", to appear in *J. Comput. Phys.*, 1995.

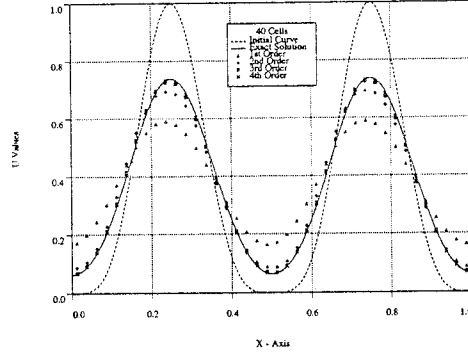


Figure 1: Linear Advection-Diffusion with ENO Interpolation ($Re = 400$)

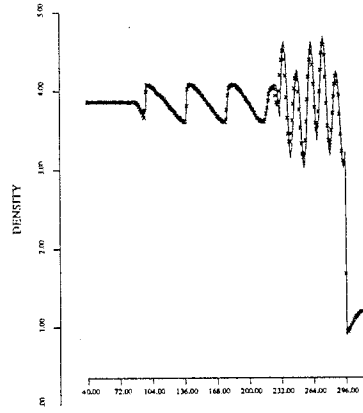


Figure 2: Shu-Osher case with 4th-order ENO reconstruction and 400 cells

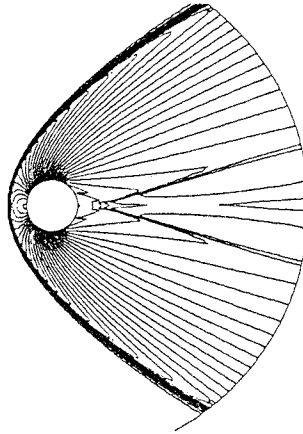


Figure 3: Density Contours for $M_\infty = 3.0$ Cylinder Case with 300×100 cells